THE JOURNAL OF BIOLOGICAL CHEMISTRY VOL. 284, NO. 29, pp. 19564–19571, July 17, 2009
Printed in the U.S.A.

GRK5 Deficiency Leads to Reduced Hippocampal Acetylcholine Level via Impaired Presynaptic M2/M4 Autoreceptor Desensitization*

Received for publication, April 9, 2009 Published, JBC Papers in Press, May 28, 2009, DOI 10.1074/jbc.M109.005959

Jun Liu[‡§], Imtiaz Rasul[‡], Yuning Sun[‡¶], Guisheng Wu[‡], Longxuan Li[‡‖], Richard T. Premont[**], and William Z. Suo[‡ ‡‡1]

*From the [‡]Laboratory for Alzheimer's Disease and Aging Research, Kansas City Veterans Affairs Medical Center, Kansas City, Missouri 64128, the [§]Department of Neurology, the Second Affiliated Hospital, Sun Yat-sen University, Guangzhou, Guangdong 510120, China, the [‡‡]Departments of Neurology and Physiology, University of Kansas Medical College, Kansas City, Kansas 66170, the [‖]Department of Neurology, Guangdong Medical College Affiliated Hospital, Zhanjian, Guangdong 524001, China, the [¶]Department of Biochemistry and Molecular Biology, Ningxia Medical University, Yinchuan, Ningxia 750004, China, and the **Department of Medicine, Duke University Medical Center, Durham, North Carolina 27710*

G protein-coupled receptor kinase 5 (GRK5) deficiency has been linked recently to early Alzheimer disease (AD), but the mechanism by which GRK5 deficiency may contribute to AD pathogenesis remains elusive. Here we report that overexpression of dominant negative mutant of GRK5 (dnGRK5) in a cholinergic neuronal cell line led to decreased acetylcholine (ACh) release. This reduction was fully corrected by pertussis toxin, atropine (a nonselective muscarinic antagonist), or methoctramine (a selective M2/M4 muscarinic receptor antagonist). Consistent with results in cultured cells, high potassium-evoked ACh release in hippocampal slices from young GRK5 knock-out mice was significantly reduced compared with wild type littermates, and this reduced ACh release was also fully corrected by methoctramine. In addition, following treatment with the nonselective muscarinic agonist oxotremorine-M, M2, and M4 receptors underwent significantly reduced internalization in GRK5KO slices compared with wild type slices, as assessed by plasma membrane retention of receptor immunoreactivity, whereas M1 receptor internalization was not affected by loss of GRK5 expression. Moreover, Western blotting revealed no synaptic or cholinergic degenerative changes in young GRK5 knock-out mice. Altogether, these results suggest that GRK5 deficiency leads to a reduced hippocampal ACh release and cholinergic hypofunction by selective impairment of desensitization of presynaptic M2/M4 autoreceptors. Because this nonstructural cholinergic hypofunction precedes the hippocampal cholinergic hypofunction associated with structural cholinergic degeneration and cognitive decline in aged GRK5 knock-out mice, this nonstructural alteration may be an early event contributing to cholinergic degeneration in AD.

G protein-coupled receptor kinase-5 (GRK5)[2] is one of the seven GRK family members whose primary function is to desensitize G protein-coupled receptors (GPCRs) (1, 2). We recently reported that increased soluble β-amyloid decreases membrane (functional) levels of GRK5 *in vitro*, and this membrane GRK5 deficiency occurs *in vivo* as well in an Alzheimer disease (AD) transgenic model (3) and in postmortem human AD brain samples (4). Moreover, the aged GRK5 knock-out (GRK5KO) mouse, which models this GRK5 deficiency in the absence of exogenous mutant human β-amyloid precursor protein (β-APP) or any other known AD-related genes (*i.e.* presenilins or tau), develops axonal defects and mild cholinergic degeneration with associated amnestic mild cognitive impairment (5). When Swedish mutant βAPP is overexpressed in the GRK5KO mice by cross-breeding with Swedish APP transgenic mice, the aged double mutant mice display significantly exaggerated brain inflammation (6). These accumulating data strongly suggest that GRK5 deficiency significantly contributes to AD pathogenesis, although the precise molecular mechanisms remain to be delineated.

Mounting evidence indicates that the substrate spectrum of broadly expressed GRKs (*i.e.* GRK2/3/5/6) can significantly overlap for some receptors, suggesting that a lack of one of these members may have only a limited impact on GPCR regulation (2). On the other hand, compensation for loss of a particular GRK member by others *in vivo* can be incomplete or selective for other receptor types. For example, GRK2KO and GRK6KO mice have been shown to display selective impairments of adrenergic and dopaminergic receptor desensitization, respectively (7, 8). Findings from different GRK isoform-targeted animals strongly support the conclusion that although redundancy exists between GRK isoforms, each isoform has its own selective substrates; should one GRK be deficient or inactivated, desensitization of its selective substrates will be impaired (1). For GRK5 in particular, previous studies have demonstrated that GRK5KO mice display selectively impaired desensitization of muscarinic acetylcholine receptors (mAChRs) (9, 10).

* This work was supported by grants (to W. Z. S.) from the Medical Research and Development Service, Department of Veterans Affairs, the American Federation for Aging Research, and resources from the Midwest Biomedical Research Foundation.

[1] To whom correspondence should be addressed: Laboratory for Alzheimer's Disease & Aging Research, Veterans Affairs Medical Center, 4801 Linwood Blvd., KS City, MO 64128. Tel.: 816-861-4700; Ext. 57084; Fax: 816-861-1110; E-mail: william.suo@va.gov.

[2] The abbreviations used are: GRK, G protein-coupled receptor kinase; AD, Alzheimer disease; ACh, acetylcholine; mAChR, muscarinic acetylcholine receptor; WT, wild type; PTX, pertussis toxin; oxo-M, oxotremorine-M; dn, dominant negative; GFP, green fluorescent protein; hr, humanized *Renilla*; MCS, multiple cloning site; RT, reverse transcription; GAPDH, glyceraldehyde-3-phosphate dehydrogenase; HACT, high affinity choline transporter; ChAT, choline acetyltransferase; VAChT, vesicular acetylcholine transporter; ICC, immunocytochemistry; CI, cholinesterase inhibitor.

To date, five mAChR subtypes have been identified, with M1, M3, and M5 receptors being $G_{q/11}$-coupled, and M2 and M4 receptors being $G_{i/o}$-coupled (11). In hippocampal memory circuits, M2 receptor (M2R) is primarily a presynaptic autoreceptor that inhibits ACh release (12, 13), whereas M1R is postsynaptic and is believed to be critical in memory processes involving an interaction between the cerebral cortex and hippocampus (11). In AD, there is a selective loss of cholinergic neurons that leads to a cholinergic hypofunction, primarily a hypoactivity of postsynaptic nicotinic and M1 muscarinic receptors (14). GRK5KO mice, when challenged with nonselective muscarinic agonists, display augmented hypothermia, hypoactivity, tremor, and salivation, as well as antinociceptive changes (9). These behavioral changes are typical M2 and/or M4 receptor-mediated functions, according to the findings from muscarinic receptor subtype knock-out mice (11, 15). Therefore, GRK5 deficiency *in vivo* may selectively impair M2/M4R desensitization. If so, the resulting presynaptic M2/M4R hyperactivity would overly inhibit ACh release from cholinergic neurons and eventually compromise the learning and memory function. This study was undertaken to investigate the impact of GRK5 deficiency on ACh release and desensitization of mAChR subtypes using GRK5-deficient models both *in vitro* and in hippocampal slices from the GRK5KO mice.

EXPERIMENTAL PROCEDURES

Materials—[Methyl-^{3}H]Choline chloride was from Amersham Biosciences. Fetal bovine serum was from Atlanta Biologicals (Norcross, GA). Pertussis toxin (PTX), methoctramine tetrahydrochloride (MT), atropine, Eserine, and oxotremorine-M (oxo-M) were purchased from Sigma. Other routine biochemical and cell culture reagents and supplies were purchased from Sigma, Invitrogen, or Fisher.

Plasmid Constructs—The coding sequence of K215R dominant negative (dn) mutant bovine GRK5 cDNA in the previously constructed pRK5-GRK5^{K215R} plasmid (16) was initially used as a template for PCR with T7 primer and a modified GRK5 reverse primer (5′-AAATTTGTCGACGCTGCTTC-CGGTGGAGTT-3′) that eliminated the stop codon of the GRK5 and added SalI site. The resultant PCR product containing the dnGRK5 and phrGFP-C mammalian expression vector (Stratagene, La Jolla, CA) were digested with BamHI/SalI and then ligated to generate dnGRK5GFP fusion construct, with the humanized *Renilla* green fluorescent protein (hrGFP) tagged at C-terminal of the dnGRK5. The point mutation of the dnGRK5GFP was then corrected by mutagenesis to generate the wild type (wt) GRK5GFP fusion construction. The full length of both the dnGRK5GFP and wtGRK5GFP fusions was sequenced to exclude any unexpected mutations.

Because of very low levels of intrinsic M2R expression in the HT22 cells, this study used pVITRO1 multigenic expression vector (InvivoGen, San Diego, CA) to coexpress the GRK5GFP along with M2 together. The pVITRO1 carries two elongation factor 1α promoters from rat and mouse origins (rEF1α and mEF1α). Similarly to their human counterpart, both promoters display strong activities that yield similar levels of expression. The *hph* gene confers resistance to hygromycin B in both *Escherichia coli* and mammalian cells. Therefore, pVITRO1 plasmids allow ubiquitous and constitutive coexpression of two genes of interest at high levels in mammalian cells. For the constructs, human M2R cDNA (University of Missouri-Rolla cDNA Resource Center) was first digested with AgeI/BglII and inserted into multiple cloning site (MCS) 2 of pVITRO1. Then the wtGRK5GFP and dnGRK5GFP fusions from the phrGFP-C vector were digested with BsiWI/AvrII and inserted into the MCS 1 of pVITRO1 (see Fig. 1*A*). For the hrGFP control, the phrGFP-C was digested with BamHI/AvrII and inserted into the MCS 1 of pVITRO1. The full length of all the inserts was sequence-confirmed before transfection.

Cell Culture and Transfection—HT22 cells are a generous gift from Dr. David Schubert (The Salk Institute, La Jolla, CA) (17, 18). The cells were cultured in Dulbecco's modified Eagles's medium supplied with 10% fetal bovine serum, 100 μg/ml streptomycin, and 100 units/ml penicillin, as previously described (19). Transfection was performed using 0.125–0.25 μg of plasmid DNA (pVITRO1-dnGRK5GFP/M2, pVITRO1-wtGRK5GFP/M2, and pVITRO1-GFP/M2) mixed with TransFast^{TM} reagents (Promega), according to the manufacturer's instruction. Forty-eight hours after transfection, hygromycin B (750 μg/ml) was added to the medium for initial selection of stably transfected cells. Two weeks after initial selection, the transfected cells were diluted and further purified with assistance of cloning cylinders (Bellco Glass, Inc., Vineland, NJ). The cloned stable lines were maintained in the culture medium containing 100 μg/ml hygromycin B to keep the selection pressure. Selected lines of HT22/dnGRK5GFP/M2, HT22/wtGRK5GFP/M2, and HT22/GFP/M2 that express equivalent numbers of the transgene copies were used for this study. For all functional assays, the HT22 cells were differentiated, as previously described (19), before any treatments were applied.

Semi-quantitative RT-PCR—The mRNA levels of cells were analyzed by RT-PCR. Total RNA was isolated from the hrGFP, wtGRK5, and dnGRK5 transfected HT22 cells using TRIzol reagent (Invitrogen) and then quantified by UV spectrophotometry (Bio-Rad). Total RNA (2 μg) was used to create cDNA using SuperScript^{TM} II first strand synthesis system kit (Invitrogen). Subsequent PCR amplification of murine GRK5, bovine GRK5GFP fusion, or GAPDH (an internal control) was carried out for 30 cycles of 94 °C for 40 s, 58 °C for 30 s, and 72 °C for 40 s, followed by a 5-min final extension at 72 °C. The PCR products were run on 1.8% agarose gels, and the intensities were measured using an image analyzer Quantity one (Bio-Rad). The primer sequences were shown in Table 1.

High K^+-evoked [^{3}H]ACh Release—This experiment was performed in both cultured cells and perfused hippocampal slices. HT22 cells seeded at a density of 5×10^5 cells/well in six-well plates were allowed for differentiation, as previously described (19). The cells were then incubated with medium containing [methyl-^{3}H]choline chloride at a final concentration of 0.05 μM (5 μCi/ml) for 2 h. This low concentration of [^{3}H]choline favors the selective uptake of choline through high affinity choline transporter (HACT) (20). After the incubation, the cells were rinsed three times, followed by high potassium (50 mM) stimulation in the presence of 1 μM Eserine (to prevent hydrolysis of the released ACh (21)) for 2 h, with normal potassium medium containing 1 μM Eserine as control for determination of basal

TABLE 1
Sequences of primers used for RT-PCR

Name	Forward sequence (5′ → 3′)	Reverse sequence (5′ → 3′)	Length
			bp
mGRK5	CAG ACG CTG ACA GCA CAG	GGA GTG AGG TAC TTG GTC AT	385
bGRK5	CTG CTC CAG AGG CTC TTC AAG[a]	CAG GAT GTC GAA GGC GAA GG[b]	320
GAPDH	CGT ATT GGG CGC CTG GTC ACC AG	GAC CTT GCC CAC AGC CTT GGC AGC	624

[a] Sequence of bovine GRK5.
[b] Sequence of hrGFP.

release. The conditioned medium (200 μl/sample) was then taken for liquid scintillation counting. As previously demonstrated, the total released radioactivity in similar conditions contains more than 90% authentic [^{3}H]ACh (13, 22). Therefore, the total secreted [^{3}H] beyond (subtracting) the basal release was used to represent the [^{3}H]ACh release in response to a treatment. For determining the impact of PTX, the differentiated cells were incubated with the medium in the absence or presence of 100 ng/ml PTX overnight before high potassium stimulation. All other treatments, such as muscarinic antagonists, were given simultaneously with the high potassium stimulation.

For the perfused brain slices, hippocampi from 3-month-old GRK5$^{+/+}$ and GRK5$^{-/-}$ mice were dissected and chopped into 300-μm slices with a McIIwain tissue chopper. After brief rinsing with cold saline, the hippocampal slices were transferred to normal potassium Hepes buffer (10.7 mM glucose, 121 mM NaCl, 25 mM $NaHCO_3$, 10 mM Hepes, 1.87 mM KCl, 1.22 mM $CaCl_2$, 1.17 mM KH_2PO_4, 1.17 mM $MgSO_4$, pH 7.4) at 37 °C, continuously gassed with 95% O_2:5%CO_2, and incubated for 45 min with buffer changing every 15 min. The [^{3}H]choline incorporation was then performed by incubation of the slices at 37 °C for 20 min in the Hepes buffer containing 0.1 μM [methyl-^{3}H]choline chloride (10 μCi/ml). Following washing with the oxygenated Hepes buffer without [^{3}H]choline, the slices were transferred to superfusion chambers and perfused (0.5 ml/min) with the oxygenated Hepes buffer without [^{3}H]choline at 37 °C for 1 h. For the purpose of predesensitizing the muscarinic receptors, one set of the slices was perfused with a saturated carbachol (1 mM) for 20 min, followed by a 20-min washing off perfusion with the oxygenated Hepes buffer. For high potassium stimulation, the isosmotic Hepes buffer containing 24 mM potassium was used. In addition, 1 μM Eserine was used along with all treatments, including normal control, high potassium, and M2 antagonist treatments, to prevent hydrolysis of the released ACh (21). Perfusion samples were collected every 2 min, with three fractions before treatment for base line and six fractions after treatment. At the end of the sample collection, the hippocampal slices were lysed, with an aliquot for protein quantification and the rest for remaining radioactivity determination. The radioactivity for all of the samples was determined by scintillation counting.

Membrane Fraction Preparation—For cultured HT22 cells, the membrane and cytosol fractions were prepared as previously described (23). Briefly, the cells were dissociated mechanically in TNT buffer (50 mM Tris-HCl, 150 mM NaCl, 0.1% Triton X-100, pH 7.6) containing 1 mM phenylmethylsulfonyl fluoride and 1× protease inhibitor mixture (Sigma). Following centrifugation at 13,000 rpm for 90 min, the supernatant was collected as the cytosol fraction. The pellet was resuspended in TNT-SDS buffer (50 mM Tris-HCl, 150 mM NaCl, 1% Triton X-100, 4 mM EDTA, 4% SDS, pH 7.4) containing 1 mM phenylmethylsulfonyl fluoride, and 1× protease inhibitor mixture. After centrifugation at 13,000 rpm for 90 min, the supernatant was collected as the membrane fraction.

The preparation of brain membrane fractions was performed according to a protocol previously described (24), with minor modifications. In brief, the brain slices were homogenized in 9× volume of prechilled homogenization buffer (50 mM Tris acetate, pH 7.4, 10% sucrose, 5 mM EDTA containing a freshly added protease inhibitor cocktails of 1 mM phenylmethylsulfonyl fluoride, 20 μg/ml benzamidine, and 20 μg/ml iodoacetamide), followed by centrifugation at 600 × *g*, 4 °C for 5 min to collect the P1 pellet (nuclear fraction). The supernatant was centrifuged at 16,000 × *g*, 4 °C for 30 min to collect the P2 pellet (mitochondria/microsome fraction). The P2 pellet was resuspended with 9× volumes of ice-cold 320 mM sucrose, followed by centrifugation at 9200 × *g*, 4 °C for 15 min to collect the P3 pellet (crude membrane/synaptosomes fraction). The pellets were then lysed with boiling denaturing lysate buffer (1% SDS, 1 mM sodium orthovanadate, 10 mM Tris-Cl, pH 7.4), supplemented with phosphatase (BioMol, Plymouth Meeting, PA) and protease inhibitor mixtures (Roche Applied Science) for routine preparation of Western blot.

Western Blotting Analyses—For the cells, differentiated or otherwise stated separately, cells at ~70% confluence were lysed with the boiling denaturing lysate buffer. For the mice, at euthanasia, cold phosphate-buffered saline-perfused brains were dissected to obtain hippocampus. Except for the cellular fraction preparation, which is described above, all other protein extract preparation, total protein content determination, Western blotting, and semi-quantitative analyses were performed as previously described (5, 19, 25). The only exception was the dilution rates for the different primary antibodies, which include synaptophysin (Sigma; 1:400), synapsin-IIa (BD Biosciences, San Jose, CA; 1:5,000), synaptotagmin (BD Biosciences; 1:1,000), SNAP-25 (BD Biosciences; 1:1,000), neuronal growth associated protein-43 (GAP-43; Sigma; 1:500), M1 and M4 (Santa Cruz Biotechnology, Santa Cruz, CA; 1:200), M2 (Santa Cruz Biotechnology; 1:100), acetylcholine esterase (Santa Cruz Biotechnology; 1:500), choline acetyltransferase (ChAT; Chemicon, Temecula, CA; 1:800), HACT (Chemicon; 1:4,000), vesicular acetylcholine transporter (VAChT; Santa Cruz Biotechnology; 1:200), hrGFP (Stratagene, La Jolla, CA; 1:5,000), and β-actin (Sigma; 1:2,500).

Immunocytochemistry (ICC)—The cells seeded onto poly-L-lysine-coated round cover-slips at a density of 1 × 10^4/well were fixed with prechilled (4 °C) 5% acetic acid in methanol for

45 min at 4 °C, followed by washing blocking and staining with specific antibodies, as previously described (25, 26).

Statistics—Quantitative data are expressed as the means ± S.E. and analyzed by analysis of variance using SPSS 11.0. Post-hoc comparisons of means were made using Scheffe's or Tukey's method where appropriate.

RESULTS

HT22 cells are immortalized murine hippocampal neuronal precursor cells. We have recently found that the differentiated HT22 neurons possess functional cholinergic neuronal properties (22). To investigate impact of GRK5 deficiency on desensitization of muscarinic receptors, we established an *in vitro* model in HT22 cells by stable transfection of K215R mutant dnGRK5. Overexpression of the dnGRK5 has been previously used to inhibit endogenous GRK5 so as to resemble GRK5 deficiency *in vitro* (16). As detailed under "Experimental Procedures," because of very low intrinsic M2R expression in HT22 cells, we inserted human M2R cDNA into the MCS2 of pVITRO1 vector and then inserted bovine dnGRK5 cDNA tagged on its C-terminal with GFP into MSC1 of the multigenic expression vector (Fig. 1*A*). In parallel, the wtGRK5GFP or GFP alone were inserted to the MSC1 of pVITRO1 and were used as controls. After transfection, selected stable lines expressing GFP/M2, dnGRK5GFP/M2, and wtGRK5GFP/M2 (for easier description, these cell lines will be abbreviated as GFP, dnGRK5, and wtGRK5, respectively) were examined using semi-quantitative RT-PCR, Western blots, and ICC. The RT-PCR result revealed that the mRNA levels of exogenous bovine dnGRK5 and wtGRK5 were similar, whereas the intrinsic murine GRK5 mRNA level in the dnGRK5 transfected cells was 24% higher than that in the wtGRK5 transfected cells. As a result, the expression levels of dnGRK5 and wtGRK5 were ~3.3- and 4.1-fold higher, respectively, than intrinsic murine GRK5 level in their corresponding cell lines (Fig. 1*B*). Western blot data confirmed that the exogenous dnGRK5GFP and wtGRK5GFP, as well as M2R, were expressed in similar levels in their corresponding cell lines. Meanwhile, expression of other intrinsic cholinergic markers of interest, such as ChAT, HACT, M1R, and M4R, were also found to be similar among the three cell lines (Fig. 1*C*). Microscopic observation further confirmed the primary cell membrane localization of both dnGRK5GFP and wtGRK5GFP fusion proteins, where GRK5 primarily localizes (1), which is in contrast to the cytosolic localization of the GFP (Fig. 2, *A*, *D*, and *G*). In addition, ICC with an antibody against M2R revealed a distribution of particle-like M2R immunoreactivity from the perinuclear region all the way to the axon terminals (Fig. 2, *B*, *E*, and *H*), which is consistent with the known cytosolic synthesis and nerve terminal distribution of M2R because of axonal transport (27, 28). In particular, at axonal terminals, the M2R immunoreactivity was found to be colocalized with dnGRK5GFP or wtGRK5GFP (Fig. 2, *C*, *F*, and *I*). These results suggest that although the GFP, dnGRK5, and wtGRK5 cell lines have different (normal, decreased, and increased, respectively) GRK5 functional status, their cholinergic properties are comparable and therefore are appropriate *in vitro* models for studying impact of GRK5 hypofunction on muscarinic neurotransmission.

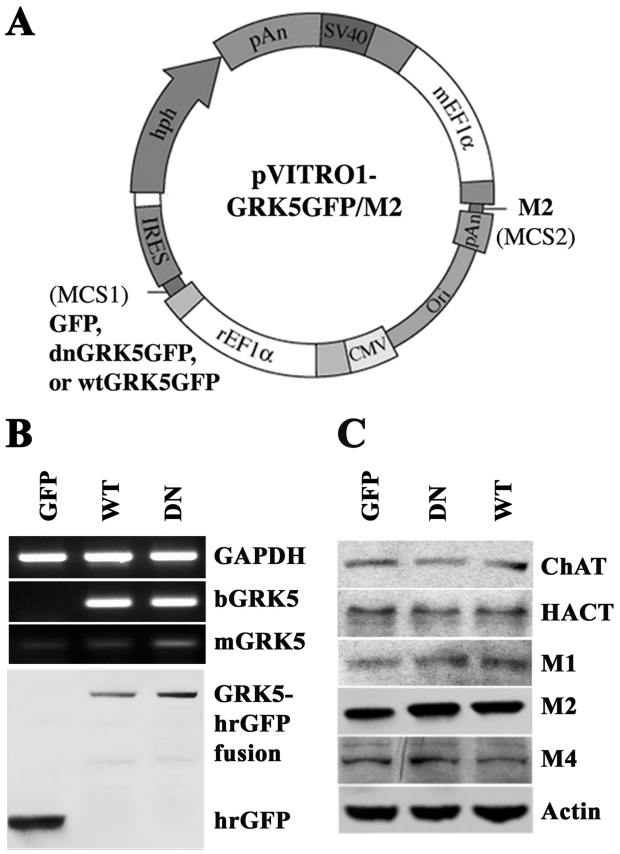

FIGURE 1. **Construction and expression of dnGRK5GFP and M2 in HT22 cells.** *A*, schematic illustration of the plasmids that contain hrGFP, bovine dnGRK5GFP, or wtGRK5GFP cDNA inserts at MCS1 and M2 cDNA at MCS2 of pVITRO1. *B*, semi-quantitative RT-PCR and Western blot characterization of dnGRK5GFP and wtGRK5GFP expression in the HT22 cells stably transfected with pVITRO1-GFP-M2, pVITRO1-dnGRK5GFP-M2, and pVITRO1-wtGRK5GFP-M2 (abbreviated as GFP, DN, and WT, respectively). bGRK5 refers to exogenous bovine GRK5; mGRK5 refers to intrinsic murine GRK5. GAPDH was used as an internal reference for RT-PCR. *C*, Western blot characterization of cholinergic markers (ChAT, HACT, M1, M2, and M4), in the GFP, dnGRK5, and wtGRK5 transfected cells. Actin was used as an internal control.

After the *in vitro* models were established, we examined high K^+-evoked ACh release from these cell lines. We found that dnGRK5 and wtGRK5 had opposite effects on [^{3}H]ACh release (Fig. 3*A*), with the former significantly decreased ($p < 0.05$) and the latter significantly increased ($p < 0.05$) compared with the GFP control cells. When these cells were pretreated with a G_i-protein activation inhibitor, PTX (100 ng/ml), all three cell lines showed severalfold increase in ACh release (Fig. 3*B*, $p < 0.001$ for all three as compared with their corresponding vehicles), but the absolute differences among the three cell lines disappeared. In addition to PTX, treatment with a nonselective muscarinic antagonist, atropine (1 μM), and a selective M2/M4R antagonist, methoctramine (MT, 100 nM), each resulted in significantly increased ACh release and also eliminated the differences among the three cell lines (Fig. 3, *C* and *D*). These results suggest that the functional difference of GRK5 in these three cell lines leads to altered ACh release, which is mediated by an altered function of PTX-sensitive G protein-coupled muscarinic M2 and/or M4 receptors.

To determine the impact of GRK5 function on internalization of mAChRs, we exposed the cells to a saturating concen-

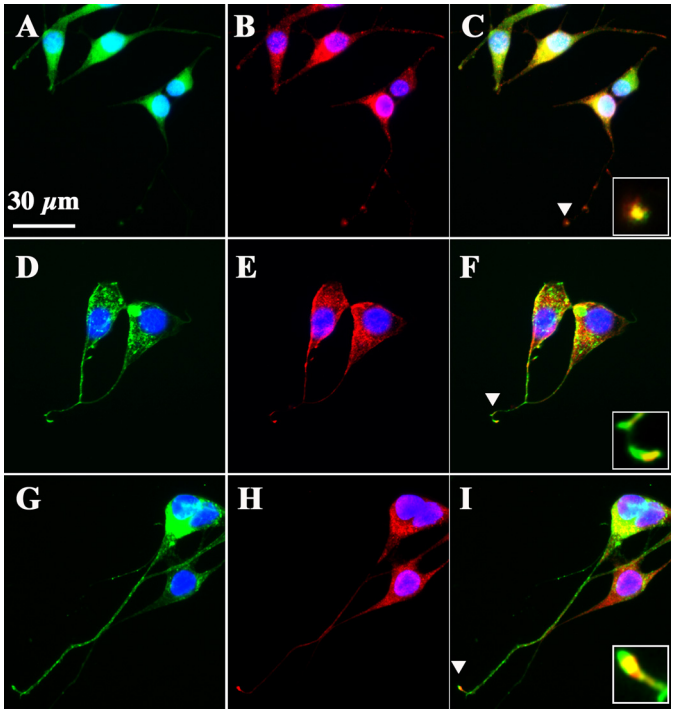

FIGURE 2. **Membrane localization of GRK5GFP fusion proteins and their colocalization with M2 at synaptic terminals.** *A*, *D*, and *G*, representative images of the expression and subcellular distribution of GFP, dnGRK5GFP, and wtGRK5GFP fusions in the GFP, dnGRK5, and wtGRK5 cell lines, respectively. *B*, *E*, and *H*, representative images of ICC staining with antibody to M2 (*red*) in the GFP, dnGRK5, and wtGRK5 cell lines, respectively. *C*, *F*, and *I*, merged panels for GFP imaging and M2 ICC staining in the GFP, dnGRK5, and wtGRK5 cell lines, respectively. The *insets* in *C*, *F*, and *I* show the high power views of the overlap of GFP imaging and M2 ICC staining at synaptic terminals as indicated by the *arrowheads*. 4′,6-Diamidino-2-phenylindole (*blue*) stains all nuclei. The *scale bar* in *A* is for all panels (30 μM).

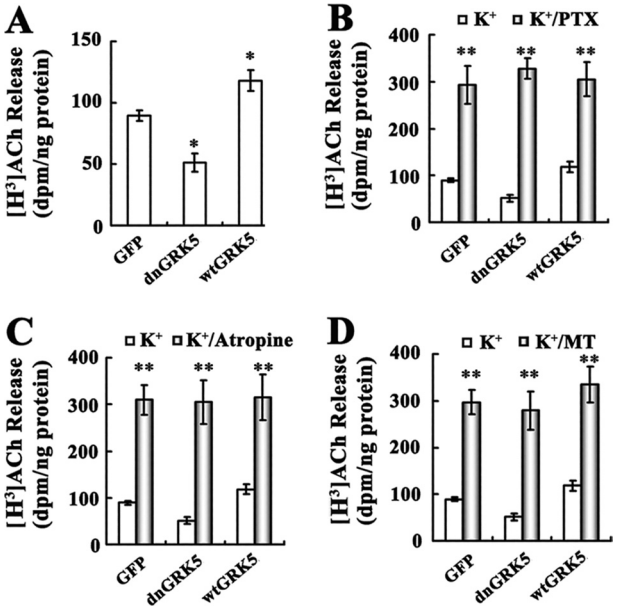

FIGURE 3. **Effects of PTX and muscarinic antagonists on high potassium-evoked [^{3}H]ACh release from the GRK5 deficient HT22 cells.** *A*, high K^+-evoked [^{3}H]ACh release in the GFP, dnGRK5, and wtGRK5 cells. A single optimal concentration of potassium (50 mM) was used to evoke the [^{3}H]ACh release ($n \geq 3$). *, $p < 0.05$, as compared with the GFP cells. *B–D*, show the effects of PTX (100 ng/ml), atropine (1 μM), and MT (100 nM) on the ACh release in the GFP, dnGRK5, and wtGRK5 cells, respectively. **, $p < 0.001$, as compared with the potassium-alone treated vehicles.

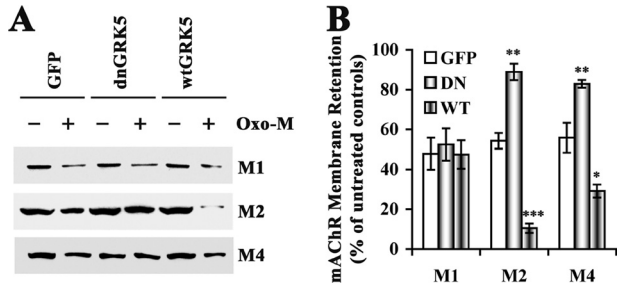

FIGURE 4. **Membrane retention of M1, M2, and M4 receptors in the GRK5 deficient HT22 cells.** The dnGRK5 cells, along with the GFP and wtGRK5 control cells, were treated with a saturation concentration of oxo-M (5 mM) before the membrane proteins were separated for Western blotting analysis. *A*, representative Western blots for M1, M2, and M4 receptors in the membrane fraction in the presence and absence of the saturated oxo-M challenge. *B*, the semi-quantification of the Western blotting results. The data were expressed as the percentage of the receptors remained in the membrane after the oxo-M treatment (the treated divided by the untreated) ($n \geq 3$). Separate one-way analysis of variance for M1, M2, and M4, respectively, revealed significant membrane retention of M2 and M4 ($p < 0.01$ for both), but not M1, in the GRK5-deficient dnGRK5 cells. In the contrast, the wtGRK5-overexpressing cells displayed significant less membrane retention of M2 ($p < 0.001$) and M4 ($p < 0.05$), but not M1, as compared with the GFP control cells. *, $p < 0.05$; **, $p < 0.01$, and $p < 0.001$, as compared with the corresponding GFP controls.

tration of oxo-M (a nonselective muscarinic agonist, 5 mM) for 20 min and then examined membrane retention of M1, M2 and M4 receptors by Western blot. We found that after oxo-M stimulation, M1 receptor remaining on the membrane in the GFP, dnGRK5 and wtGRK5 HT22 cells was equivalent (Fig. 4). However, the remaining membrane M2 and M4 receptors were significantly higher in the dnGRK5 cells ($p < 0.01$ for both M2 and M4) but lower in the wtGRK5 cells ($p < 0.001$ for M2 and $p < 0.05$ for M4), as compared with those in the GFP cells. In addition, we also found that following oxo-M stimulation, cytosolic (internalized) M2 and M4, but not M1, were lower in the dnGRK5 cells and higher in the wtGRK5 cells as compared with those in the GFP cells (data not shown), which is consistent with the higher membrane retention of M2 and M4 in the dnGRK5 cells and the lower membrane M2 and M4 in the wtGRK5 cells. Taken together, these results suggest that overexpression of dnGRK5 impaired the agonist-induced internalization of M2 and M4 but not M1 receptors, whereas overexpression of wtGRK5 had the opposite effects.

Comparison of *in vitro* and *in vivo* assays demonstrate clearly that selectivity of GRK regulation of GPCR substrates is a function of specific cellular contexts (29). Therefore, to validate the physiological relevance of our *in vitro* findings, we also performed experiments in an *ex vivo* setting, using acute hippocampal slice cultures from young adult GRK5KO mice. First, hippocampal tissues from female GRK5KO and WT littermates were used for Western blotting analyses to determine whether levels of cholinergic and synaptic markers in these animals are compatible. The examined molecules included ChAT, acetylcholine esterase, HACT, VAChT, M1R, M2R, M4R, synaptophysin, synapsin II, synaptotagmin, SNAP-25, and GAP-43. Unlike the decreased levels of some of these markers that we have reported in aged GRK5KO mice (5), young GRK5KO mice displayed comparable levels of both cholinergic and synaptic markers as compared with WT littermates (Fig. 5). These data suggest that the hippocampal cholinergic system in 3-month-

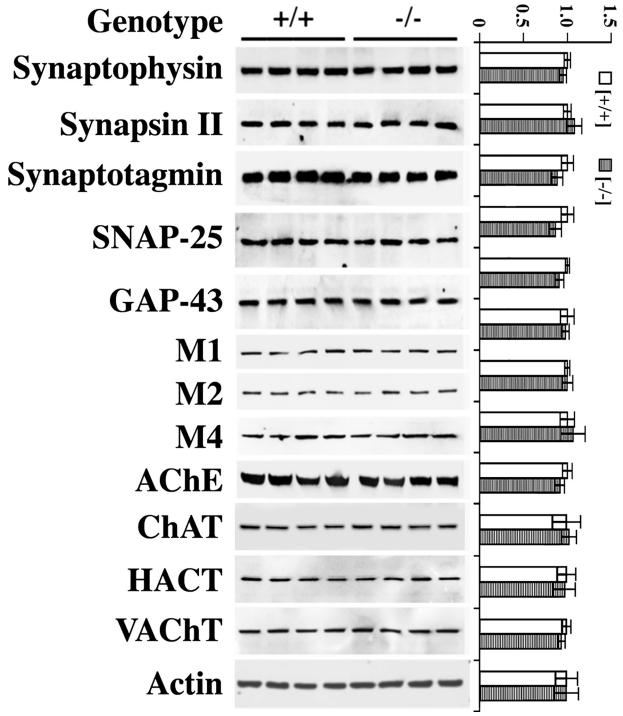

FIGURE 5. **Expression of synaptic and cholinergic markers in the young adult GRK5KO mice.** Levels of synaptic and cholinergic markers in the 3-month-old GRK5KO mouse brains were analyzed by Western blotting using antibodies against synaptophysin, synapsin II, synaptotagmin, SNAP-25, GAP-43, M1, M2, M4, acetylcholine esterase, ChAT, HACT, and VAChT. The representative blots were shown on the *left*, and the corresponding semi-quantitative results ($n = 4$) are plotted on the *right*. The results revealed no significant changes for any of the examined molecules, suggesting that the cholinergic system in these young animals is normal at the structural level.

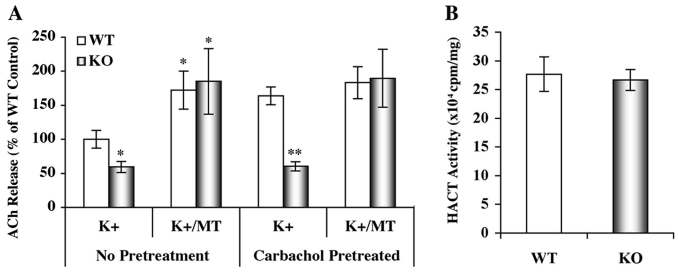

FIGURE 6. **Reduced ACh release in the hippocampal slices of the young adult GRK5KO mice.** The high K^+-evoked [^{3}H]ACh release from the hippocampal slices of 3-month-old GRK5$^{-/-}$ (KO, $n = 3$) and GRK5$^{+/+}$ (WT, $n = 5$) mice were measured as described under "Experimental Procedures." *A*, ACh release from the hippocampal slices of the young adult GRK5KO mice. The slices were separated into two parallel groups, with one group pretreated with a saturated concentration of carbachol (1 mM) to desensitize the muscarinic receptors, and with the other group as nontreated control. The ACh release was stimulated with high potassium (24 mM) in the presence and absence of 20 nM MT. We found that the GRK5KO mice displayed ~40% ($p < 0.05$) and 65% ($p < 0.01$) less ACh release than the WT mice in the cases of without and with the predesensitization, respectively. In either case, however, coperfusion of MT eliminated the differences between the GRK5KO and WT. *, $p < 0.05$; **, $p < 0.01$, as compared with the corresponding K^+-alone treated WT controls. *B*, the total HACT activity was estimated by measuring the total uptake of [^{3}H] into the slices. The results revealed no difference between the GRK5KO and WT mice.

old GRK5KO mice is normal at the structural level, and cross-strain comparisons can be made directly to measure differences in cholinergic function independent of gross structural alterations.

To determine cholinergic function, we used high K^+-evoked [^{3}H]Ach release from hippocampal slices. We found that the ACh release from GRK5KO hippocampal slices was ~40% lower than from WT slices ($p < 0.05$) and that the M2/M4R antagonist methoctramine (20 nM) not only increased ACh release from both the WT and GRK5KO but also fully corrected the difference between GRK5KO and WT (Fig. 6*A*). Moreover, when the hippocampal slices were pretreated with a saturating concentration of the nonselective muscarinic agonist carbachol (1 mM), we found that the difference in high K^+-evoked [^{3}H]ACh release between the WT and GRK5KO became more dramatic ($p < 0.01$), because of increased ACh release from the WT but not from the GRK5 knock-out tissue. When coperfused with 20 nM methoctramine, high K^+ evoked ACh release from the WT slices did not increase further compared with K^+ alone, but the ACh release from GRK5KO increased significantly compared with K^+ alone to the level equivalent to that in the K^+-treated WT (Fig. 6*A*). In addition to ACh release, we also examined the total [^{3}H]choline uptake by the WT and GRK5KO hippocampal slices, and we found no difference between them (Fig. 6*B*), suggesting that the difference in ACh release between the WT and GRK5KO cannot be attributed to an alteration of choline reuptake activity. Because hippocampal M2/M4 receptors are primarily presynaptic autoreceptors that inhibit ACh release (12, 13), these results suggest that the GRK5 deficiency leads to a significant reduction of hippocampal ACh release through an impaired desensitization of M2 and/or M4 receptors.

To further investigate the effect of GRK5 on mAChRs *in vivo*, we also examined membrane retention of M1, M2, and M4 receptors after treatment with a saturating dose of carbachol in hippocampal slices. After treatment with 1 mM carbachol for 20 min, the slices were fractionated to obtain P1 (nuclear), P2 (mitochondria and microsomes), and P3 (crude membrane) pellet fractions. Western blots revealed that there were no differences for either P1 and P3 fractions between the WT and GRK5KO in any cases but that the membrane fraction (P3) showed significantly more retention in the GRK5KO for M2R ($p < 0.001$, as compared with the WT) and M4R ($p < 0.05$, as compared with the WT), but not for M1R (Fig. 7). These results suggest that the GRK5 deficiency *in vivo* robustly impairs the internalization of M2R and to a slightly lesser extent affects M4R but has no effect on M1 receptor.

DISCUSSION

Because GRK-mediated phosphorylation of a receptor leads both to receptor desensitization (uncoupling from G protein activation) and to receptor sequestration (internalization from the cell surface into endosomal vesicles) through the same mechanism (promoting receptor association with β-arrestin proteins) (1, 29), we used agonist-stimulated receptor internalization as a surrogate measure for GRK-mediated receptor desensitization.

This study utilized an *in vitro* model, HT22 cholinergic neurons that overexpress kinase-inactive dnGRK5, and an *ex vivo* model, hippocampal slices from GRK5KO mice, to mimic functional GRK5 deficiency and investigated effects of the GRK5 deficiency on ACh release and desensitization of M1, M2, and M4 muscarinic receptors. In the *in vitro* model, the K215R

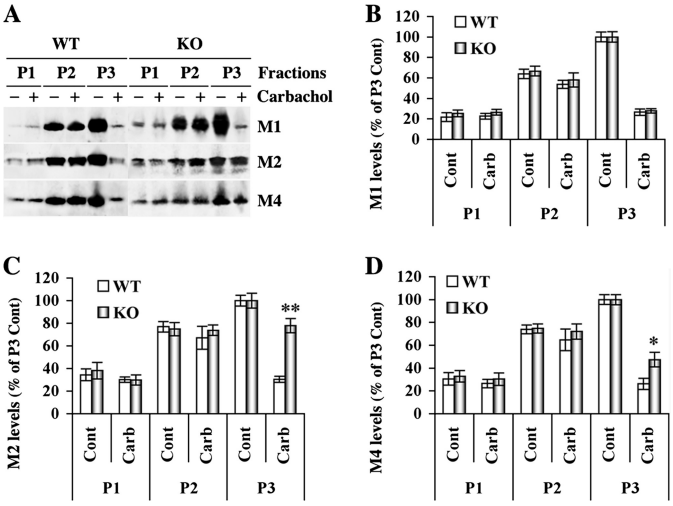

FIGURE 7. **Membrane retention of M1, M2, and M4 receptors in the young adult GRK5KO mice.** Cortical slices from the 3-month-old GRK5 KO mice were treated with the saturated carbachol (*Carb*, 1 mM) in the oxygenated Kreb's buffer at 37 °C for 20 min and then subjected to multi-step homogenization and centrifugations to isolate subcellular fractions, including pellets for nuclear (*P1*), mitochondria/microsome (*P2*), and crude membrane/synaptosome (*P3*). Equal amount (50 μg/lane) of proteins were analyzed by SDS-PAGE, followed by Western blotting. *A*, representative Western blots for M1, M2 and M4. *B–D*, semi-quantification ($n = 3$) for M1, M2, and M4, respectively. All of the data were standardized against the mean of the untreated membrane fraction, and the percentages over the P3 controls (*Cont*) were plotted as shown. *, $p < 0.05$; **, $p < 0.001$, as compared with the same fraction of the WT mice.

dnGRK5 was overexpressed to compete with the intrinsic GRK5, to create a functional GRK5 deficiency (16). As a result, this functional GRK5 deficiency led to reduced ACh release, which could be corrected by preventing muscarinic receptor activation of G_i/G_o proteins (PTX) and by antagonizing all muscarinic receptors (atropine) or just M2/M4 receptors (methoctramine). Moreover, the GRK5 deficiency also resulted in an impaired internalization of M2 and M4 but not M1 receptors, in response to saturating treatment with the nonselective muscarining agonist oxotremorine-M. It is known that M2R and M4R function as presynaptic autoreceptors in hippocampal cholinergic neurons to inhibit ACh release (12, 13). In addition, activation of these receptors leads to the receptor desensitization and internalization by either GRKs or other kinases (1, 2). Therefore, the impaired internalization of M2/M4R in the dnGRK5 cells indicates that a sufficient amount of fully functional GRK5 is essential for the desensitization and internalization of M2/M4 receptors in these cells. Taken together, these *in vitro* results suggest that the functional GRK5 deficiency in the HT22 hippocampal cholinergic neuronal model leads to decreased ACh release through a selective impairment of M2/M4 receptor desensitization/internalization.

Based on the *in vitro* findings, we went further to determine effects of the GRK5 deficiency on ACh release and desensitization of M1, M2, and M4 receptors in an *ex vivo* model, hippocampal slices from GRK5KO mice. Aged GRK5KO mice displayed mild cholinergic and synaptic degenerative changes (5). Therefore, without correction of their structural abnormalities, it is impropriate to directly compare the cholinergic functional difference between aged WT and GRK5KO mice. In the 3-month-old GRK5KO mice, however, our characterization indicates that these young adults had normal levels of cholinergic and synaptic markers as compared with age-matched WT animals, and therefore these younger mice are suitable for direct comparison of cholinergic functions. Using the hippocampal slices from these young animals, we found a significant reduction in ACh release in response to high K^+ stimulation in the GRK5KO mice. Consistent with the *in vitro* findings, the reduced ACh release was fully corrected by the M2/M4 receptor antagonist, methoctramine. In parallel, we desensitized the muscarinic receptors with a saturating dose of carbachol before high K^+ stimulation and found that WT slices released significantly more ACh (because of reduced autoreceptor inhibition of release) but that the inhibited ACh release in the GRK5KO mice remained (consistent with undesensitized autoreceptors). Again, the difference between the WT and GRK5KO was corrected by methoctramine treatment. Furthermore, when the carbachol-desensitized slices were fractionated, we found retention of membrane M2R and membrane M4R in the GRK5KO samples compared with WT samples, consistent with a failure to internalize after receptor activation. These results together strongly suggest that GRK5 deficiency selectively impairs M2 and M4 receptor desensitization/internalization both *in vitro* and *in vivo*, and the consequence of this impaired desensitization of presynaptic M2/M4 receptors is prolonged inhibitory M2/M4 receptor signaling, which leads to reduced ACh release and an overall hippocampal cholinergic hypofunction.

Cholinergic hypofunction is one of the key neurochemical changes in AD. It is worth noting that the "cholinergic hypofunction" conventionally refers to reduced cholinergic activity associated with cholinergic neuronal degeneration or postsynaptic M1 and nicotinic degenerative changes (14). Here we show a clear presynaptic cholinergic hypofunction in the absence of degenerative changes. We have previously observed that the aged GRK5KO mice displayed mild cholinergic and synaptic degenerative changes (5). In this study, we showed that the hippocampal cholinergic hypofunction can occur without obvious structural degenerative changes, and this hippocampal cholinergic hypofunction without structural degeneration in young mice precedes hypofunction with structural degeneration in aged GRK5KO mice. Therefore, it raises the question of whether the latter is a direct consequence of the former.

We have previously shown that GRK5 deficiency is associated with soluble β-amyloid accumulation in AD (4). Now we find that the hippocampal cholinergic hypofunction directly results from GRK5 deficiency. Moreover, the hippocampal cholinergic hypofunction in the GRK5KO mice can be corrected by a selective M2/M4 antagonist, indicating that resynaptic M2/M4 autoreceptors may be valuable therapeutic targets in AD, at least in the sense of combating the cholinergic hypofunction in AD.

Among the FDA-approved AD medications are mainly cholinesterase inhibitors (CIs) that aim at halting the ACh degradation at the synaptic clefts. Although the CIs are expected to increase the ACh concentration at synaptic clefts and enhance the postsynaptic cholinergic activities, the increased ACh should also act on presynaptic autoreceptors to inhibit further ACh release. The latter effect, as demonstrated in this study, is

dramatically enhanced in the presence of functional GRK5 deficiency, as in AD. The sustained presynaptic inhibitory effect may lead to an opposite consequence to what the CIs were originally designed for and could have adverse effects on patients in long term, especially if functional cholinergic deficiency can lead to later cholinergic degeneration. Therefore, further studies are warranted to clarify whether CI drugs indeed exacerbate presynaptic M2/M4 hyperactivity and lead to a sustained inhibition of ACh release and whether the addition of an M2/M4 receptor antagonist in addition to the CIs gives an improved outcome for combating the cholinergic hypofunction in AD.

Acknowledgment—We sincerely thank Dr. Robert J. Lefkowitz (Duke University)for providing the original GRK5KO mouse breeding pairs, consultations, and review of this manuscript.

REFERENCES

1. Kohout, T. A., and Lefkowitz, R. J. (2003) *Mol. Pharmacol.* **63,** 9–18
2. Pitcher, J. A., Freedman, N. J., and Lefkowitz, R. J. (1998) *Annu. Rev. Biochem.* **67,** 653–692
3. Suo, Z., Wu, M., Citron, B. A., Wong, G. T., and Festoff, B. W. (2004) *J. Neurosci.* **24,** 3444–3452
4. Suo, Z., Wu, M., Citron, B. A., Wong, G. T., and Festoff, B. W. (2005) *Neurobiol. Aging* **25,** S2–291
5. Suo, Z., Cox, A. A., Bartelli, N., Rasul, I., Festoff, B. W., Premont, R. T., and Arendash, G. W. (2007) *Neurobiol. Aging* **28,** 1873–1888
6. Li, L., Liu, J., and Suo, W. Z. (2008) *J. Neuroinflammation* **5,** 24
7. Jaber, M., Koch, W. J., Rockman, H., Smith, B., Bond, R. A., Sulik, K. K., Ross, J., Jr., Lefkowitz, R. J., Caron, M. G., and Giros, B. (1996) *Proc. Natl. Acad. Sci. U.S.A.* **93,** 12974–12979
8. Gainetdinov, R. R., Bohn, L. M., Sotnikova, T. D., Cyr, M., Laakso, A., Macrae, A. D., Torres, G. E., Kim, K. M., Lefkowitz, R. J., Caron, M. G., and Premont, R. T. (2003) *Neuron* **38,** 291–303
9. Gainetdinov, R. R., Bohn, L. M., Walker, J. K., Laporte, S. A., Macrae, A. D., Caron, M. G., Lefkowitz, R. J., and Premont, R. T. (1999) *Neuron* **24,** 1029–1036
10. Walker, J. K., Gainetdinov, R. R., Feldman, D. S., McFawn, P. K., Caron, M. G., Lefkowitz, R. J., Premont, R. T., and Fisher, J. T. (2004) *Am. J. Physiol. Lung Cell Mol. Physiol.* **286,** L312–319
11. Matsui, M., Yamada, S., Oki, T., Manabe, T., Taketo, M. M., and Ehlert, F. J. (2004) *Life Sci.* **75,** 2971–2981
12. Levey, A. I. (1996) *Proc. Natl. Acad. Sci. U.S.A.* **93,** 13541–13546
13. Zhang, W., Basile, A. S., Gomeza, J., Volpicelli, L. A., Levey, A. I., and Wess, J. (2002) *J. Neurosci.* **22,** 1709–1717
14. Terry, A. V., Jr., and Buccafusco, J. J. (2003) *J. Pharmacol. Exp. Ther.* **306,** 821–827
15. Wess, J. (2004) *Annu. Rev. Pharmacol. Toxicol.* **44,** 423–450
16. Pitcher, J. A., Fredericks, Z. L., Stone, W. C., Premont, R. T., Stoffel, R. H., Koch, W. J., and Lefkowitz, R. J. (1996) *J. Biol. Chem.* **271,** 24907–24913
17. Li, Y., Maher, P., and Schubert, D. (1997) *Neuron* **19,** 453–463
18. Li, Y., Maher, P., and Schubert, D. (1998) *Proc. Natl. Acad. Sci. U.S.A.* **95,** 7748–7753
19. Suo, Z., Wu, M., Citron, B. A., Palazzo, R. E., and Festoff, B. W. (2003) *J. Biol. Chem.* **278,** 37681–37689
20. Pittel, Z., Heldman, E., Rubinstein, R., and Cohen, S. (1990) *J. Neurochem.* **55,** 665–672
21. Gifford, A. N., Bruneus, M., Gatley, S. J., Lan, R., Makriyannis, A., and Volkow, N. D. (1999) *J. Pharmacol. Exp. Ther.* **288,** 478–483
22. Liu, J., Li, L., and Suo, W. Z. (2009) *Life Sci.* **84,** 267–271
23. Li, L., Rasul, I., Liu, J., Zhao, B., Tang, R., Premont, R. T., and Suo, W. Z. (2009) *Brain Res. Bull.* **78,** 145–151
24. Rogers, S. W., Hughes, T. E., Hollmann, M., Gasic, G. P., Deneris, E. S., and Heinemann, S. (1991) *J. Neurosci.* **11,** 2713–2724
25. Suo, Z., Wu, M., Citron, B. A., Gao, C., and Festoff, B. W. (2003) *J. Biol. Chem.* **278,** 31177–31183
26. Suo, Z., Wu, M., Ameenuddin, S., Anderson, H. E., Zoloty, J. E., Citron, B. A., Andrade-Gordon, P., and Festoff, B. W. (2002) *J. Neurochem.* **80,** 655–666
27. Guidry, G., Willison, B. D., Blakely, R. D., Landis, S. C., and Habecker, B. A. (2005) *Auton Neurosci.* **123,** 54–61
28. Amadeo, A., Arcelli, P., Spreafico, R., and De Biasi, S. (1995) *Neurosci. Lett.* **184,** 161–164
29. Premont, R. T., and Gainetdinov, R. R. (2007) *Annu. Rev. Physiol.* **69,** 511–534